Optimal Energy Management Strategies of a Parallel Hybrid Electric Vehicle Based on Different Offline Optimization Algorithms

Marwa Ben Ali*‡, Ghada Boukettaya**

* Electrical Engineering Department, Laboratory of Electrical Systems and Renewable Energies (SEER), University of Gabes, National Engineering School of Gabes (ENIG), 6029 Gabes, Tunisia
** Electrical Engineering Department, Laboratory of Electrical Systems and Renewable Energies (SEER), University of Sfax, National Engineering School of Sfax (ENIS), 3038 Sfax, Tunisia

(Benali.marwa15@gmail.com, ghada.boukettaya@enis.tn)

‡ Corresponding Author; Marwa Ben Ali, 3039 Sfax, Tel: +21695765051,

Fax: +21695765051, Benali.marwa15@gmail.com

Received: 28.09.2020 Accepted:30.10.2020

Abstract- The optimization of energy consumption applied to the hybrid electric vehicle (HEV) with a parallel architecture seems to be one of the important challenges to decrease fuel consumption and CO_2 emission in the world. For this reason, this study aimed to develop a comparative study between different offline optimization algorithms to ensure an optimal power split between the electric motor (EM) and the internal combustion engine (ICE) mainly in the hybrid propulsion mode. In this approach, the energy management strategy is divided into two sections. The first is a supervision study that plays an essential role in operating mode switching of the traction system. The second consists of the objective function definition involved the fuel consumption cost, electric charge cost, and components cost as well as the optimization algorithms presentation. The problem formulation was implemented using MATLAB/Simulink software and evaluated under the Normalized European Drive Cycle (NEDC). Results related to fuel consumption, CO_2 emission, computational time, best cost, and SOC sustaining operation were compared. Thus, the results obtained from MATLAB simulation proved the effectiveness of used algorithms with 6.53% to 46.43% fuel economy saving.

Keywords Hybrid electric vehicle, Power management strategy, Offline optimization, NEDC drive cycle, Objective function.

1. Introduction

The intensive global fuel consumption in the transport sector has led to a high CO_2 emission [1], which resulted in horrible global warming that seriously threatens the world [2]. Consequently, humanity faces the challenge of how to ensure the best global energy balance [3, 4] and to consider the climatic and ecological consequences of their consumption.

So far, the development of the electric transport industry has been proposed as one of the greatest achievements due to its relying on primary green energy sources [5, 6], especially the solar sources, which have become the most effective alternative of the non-renewable energy sources to produce the final energy [7, 8].

According to the EV outlook, the EV stock exceeded 55 million vehicles in 2025 and it will reach about 135 million vehicles in 2030. Besides, the global EV demands will arrive at 12 million in 2025 and nearly 23 million in 2030 [9].

The HEV has attracted the attention of the researchers and industries worldwide as a perfect solution to minimize CO_2 emissions and manage the energy flow between electricity and fuel consumption [10]. This huge attention is attributed to the several advantages such as the low CO_2 emission when used in the electric mode, added to its economic benefit as far as the fuel consumption is affected. This has led to the important growth of the HEV sales in such countries as Canada, Sweden and Japan [11].

The HEV is characterized by three different architectures; these are series, parallel and combined [12]. In the parallel architecture, the electric and thermal motors are mechanically linked, so that the power to the wheels can be supplied simultaneously or alternately by the two motors with minimal energy losses compared to the series one. The challenges associated with the two energy sources of the HEV involve the importance of the energy management methods and the essential role of the optimization algorithms is the fuel consumption and CO_2 emission reduction [13]. According to the literature, the optimization algorithms are split into two types: rule-based and optimizations based methods. Each method is divided into sub-types [14, 15]. The rule-based method is split into determined and fuzzy logic methods. However, the optimization-based method is divided into real-time methods such as a robust control approach and predictive control and global optimization techniques such as genetic algorithms (GA), dynamic programming (DP)… [16,17]. In the global optimization methods, the used drive cycle has to be known to find the optimal solution based on future expectations and results, contrary to the real-tie optimization method.

In the literature, different optimization algorithms have been studied. In [18], a comparison study between convex and dynamic programming (DP) algorithms to minimize the fuel consumption relying on different initial battery SOCs have been studied. However, other researchers compare the convex optimization algorithm and DP algorithm applied to a parallel PHEV based on the model size optimization [19]. In [20], an implementation of GA to optimize the total torque distribution between the motors of the vehicle then, a comparison of the results to the common control strategy. In [21], authors have deals with a comparison between two algorithms, convex and PSO, to optimize the model component sizes for the lowest cost and fuel consumption, under various performances of the PHEV. Authors in [22] have studied the PSO and the DIviding RECTangles (DIRECT) optimization algorithms under different drive cycles. Furthermore, [23, 24] can be considered as a wealth as it focuses on the review of the very recently published research papers about different optimizations algorithms definition, classifications, advantages, and some examples of applications. Researches in [25] have worked on the real time optimization algorithms with the equivalent consumption minimization strategy (ECMS) to reduce not only the total cost of parallel PHEV but also the total fuel consumption compared to the other three control strategies (Rule-based , Global optimal , Simpler real-time) under a large database of driving cycles. In [26], the authors are interested only in the optimization of PHEVs component sizing the using parallel chaos optimization algorithm (PCOA) for different all electric ranges (AER) and with two different battery types. ECMS is a novel control theory for energy management optimization applied to the HEV and compared with classical DP was studied in [27] to minimize the vehicle fuel consumption and NOx emission.

Within this framework, the primary interest of this comparative study is to ensure the feasibility, efficiency and rapidity of five offline optimization algorithms for a nonlinear problem with different constraints using the same number of iterations, populations and tolerance to satisfy the objective function. The proposed optimization algorithms are expected to minimize the objective function described by economic criteria searching the optimal motors torques needed by each motor and minimizing fuel consumption, CO_2 emission and the SOC sustaining operation and mainly the total cost of the vehicle under the NEDC cycle taking into account energy consumption, vehicle life time, distance among others. Firstly, we focused on the parallel architecture where a supervision strategy is needed to control the electric and thermal energy flow of the vehicle with five different modes. Each mode takes into account the vehicle speed and the battery SOC. Next, the energy management problem was solved offline by different optimization algorithms. Thus, values are extracted into tables, which were implemented later online in the MATLAB/Simulink software.

However, the comparative results described in this work can direct the interested users towards the best choice of the appropriate optimization algorithm according to his prefixed objectives.

The remainder of this paper is structured as follows: powertrain system model was developed in section 2, it consists of different components, a storage system, EM and ICE incorporates different converters to exchange information about energy and its flow through the different physical processes. Using the various output data, the main contribution of this study was to improve the fuel consumption minimization and CO_2 emission. In section 3, the inversion-based control was associated to the parallel HEV model. In section 4, the proposed energy flow diagram was introduced to organize the relation between all components defined in different modes. In section 5, a problem formulation of the system was detailed with different constraints and components costs. In section 6, the proposed optimization algorithms were implemented to provide an optimal solution for electricity and fuel consumption in the hybrid model. The simulation results have demonstrated that the proposed energy management system is efficient and convenient as it can conceive an optimal target configuration considering the simple negotiation strategies in section 7. The major conclusions of this article were drawn in section 8.

2. System Description and Modeling

This study aimed to point out the great efficiency of the optimization algorithms which could provide a significant reduction of the total purchase cost, fuel consumption, CO_2 emission and improvement of battery SOC sustaining charge operation of the HEVs during their road journeys under an appropriate supervision strategy. As illustrated in Fig.1 the overall system of the studied vehicle included a permanent magnet synchronous machine (PMSM), which is linked to the battery by means of a conversion system composed of a DC/AC converter.

This converter is, in turn, linked to an intermediate DC bus, and an inverter. Besides, the parallel HEV includes an ICE, which is linked to the continuous variable transmission (CVT) and the reduction gear. The vehicle run in different operating modes takes account of vehicle speed and battery SOC. The different parameters of the parallel HEV are shown in Table 1.

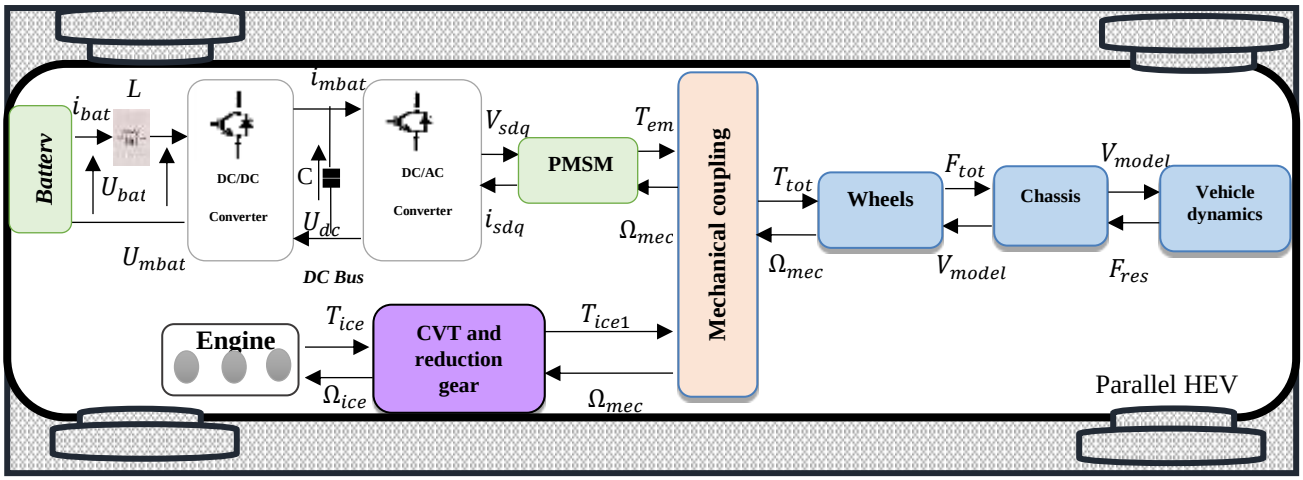

Fig.1. The studied parallel HEV system configuration.

Table 1. Different parameters of the parallel HEV system.

Components	Parameters	Symbols	Values
Vehicle	vehicle mass	m	950 kg
	Frontal surface aerodynamic × drag coefficient	SC_d	0608 m^2
	Rolling resistance coefficient	C_r	0.00904
	Gravity acceleration	g	9.81 m/s^2
	Road slope angle	α	0 rad
	The density of the air	ρ	1.125 kg/m^3
	Wheel radios	r	0.28 m
PMSM	PMSM power	P	4.5 kWh
	Pole pair	p	17
	Stator resistance	R_s	0.6 Ω
	Stator inductance	L_s	3 mh
	Rotor flux linkage	Φ_m	0.106
ICE	Maximal ICE torque	T_{icemax}	32.5 Nm
	Speed range	Ω_{ice}	0-2250 rpm
Battery	Voltage	U_{bat}	250 V
	Capacity	Q	128 Ah
Transmission: CVT and reduction gear	Initial gear ratio	i_1	2
	Final gear ratio	i_2	3

The parallel HEV system was designed to satisfy the user's demand in different driving conditions (wind, rain, low visibility and slopes…).Therefore, this system of 4.5 kW electric motor and 250 V lithium ion battery can propel the vehicle in the maximum electric range with 0.4286 degree of hybridization.

The vehicle power demand P_{dem} is modeled by the longitudinal vehicle dynamic based on the second Newton law developed in equation (1).

$$m\vec{a} = \sum \vec{F} \quad (1)$$

Where: $\vec{F}$ is the propulsion and $\vec{a}$ is the acceleration.

Different forces are acting on the vehicle body; we notice $\vec{F}_{tot}$ is the tractive force abandoned the wheels supplied by the motor and $\vec{F}_{res}$ is the resistance force [28]. Each can be expressed in the follows equations:

$$\vec{F} = \overrightarrow{F_{tot}} + \overrightarrow{F_{res}} \quad (2)$$

$$\vec{F}_{tot} = \frac{\vec{T}_{tot}}{r} \quad (3)$$

With:

$$\overrightarrow{F_{res}} = \vec{F}_r + \vec{F}_g + \vec{F}_a \quad (4)$$

Where:

- The rolling resistance force F_r is defined by :

$$F_r = mgC_r \quad (5)$$

- The aerodynamique force F_a is defined by:

$$F_a = \frac{1}{2}\rho SC_d V_{model}^2 \quad (6)$$

Where: V_{model} is the parallel HEV model speed.

- The gravity force F_g is defined by :

$$F_g = mg\sin(\alpha) \tag{7}$$

2.1. Chassis modeling

Vehicle chassis is the main support of the vehicle structure where all other components are attached. It has the role of different force treatment. The chassis model is presented by the following equation:

$$F_{tot} - F_{res} = m\frac{dV_{model}}{dt} \tag{8}$$

2.2. Wheels modeling

The mechanical wheels speed Ω_{mec} can be calculated using the following equation:

$$\Omega_{mec} = \frac{V_{model}}{r} \tag{9}$$

2.3. PMSM motor modeling

There are many types of electric motors that can be used in a hybrid electric vehicle such as induction motor (IM), DC motor, switching reluctance motor (SRM) and PMSM motor. The choice of the motor depends on many factors such as cost, efficiency, mass, volume and maintenance. However, the PMSM is the used motor for the vehicle basing on its efficiency, low maintenance and low cost. In addition, the PMSM is the most adapted machine in the literature studies.
Its direct and quadrature currents i_{sd} and i_{sq} model respectively in the Park reference frame are given by the following equation (10):

$$\frac{d}{dt}\begin{pmatrix} i_{sd} \\ i_{sq} \end{pmatrix} = \begin{pmatrix} \frac{-R_s}{L_s} & \frac{p\Omega_{mec}L_s}{L_d} \\ \frac{-R_s}{L_s} & \frac{-p\Omega_{mec}L_s}{L_s} \end{pmatrix}\begin{pmatrix} i_{sd} \\ i_{sq} \end{pmatrix} + \begin{pmatrix} \frac{1}{L_s} \\ \frac{1}{L_s} \end{pmatrix}\begin{pmatrix} v_{sd} \\ v_{sq} \end{pmatrix} + \begin{pmatrix} 0 \\ -p\Omega_{mec}\Phi_m \end{pmatrix} \tag{10}$$

The electromagnetic torque T_{em} applied by the EM to the parallel HEV is given by the fundamental equation as follows [29]:

$$T_{em} = p\Phi_m i_{sq} \tag{11}$$

Figure 2 describes the curve of the maximum torque-speed of the PMSM at various operating points. However, the analytical results of the motor power losses with the simulation at different speeds and torque points are illustrated in Fig.3.

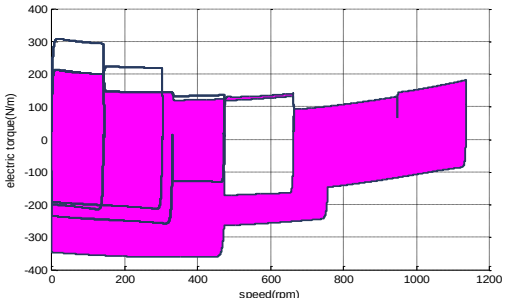

Fig.2. Curve of the PMSM torque-speed.

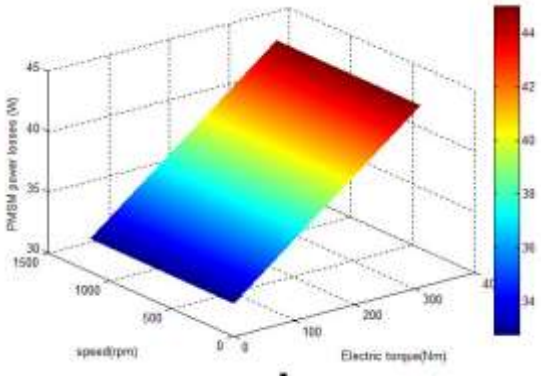

Fig.3. PMSM power losses.

2.4. DC bus modeling

The DC voltage equation can be written as:

$$U_{dc} = \frac{1}{C}\int i_{dc}dt \tag{12}$$

Where: i_{dc} and C are the current and the capacity of the DC bus.
The current of the DC bus can be written as:

$$i_{dc} = i_{bat} - i_m \tag{13}$$

Where: i_{bat} is the battery current and i_m is the current through the converter.

2.5. Lithium ion Battery modeling

The parallel HEV as described in Fig.1 includes a storage system, which consists of a DC/DC converter connected to an inductor filter between the battery and the DC bus and a bidirectional inverter [7].

Thus, the transport sector requires batteries with high performance, perfect autonomy and long service life to reduce costs and preserve the longevity of the vehicle [30]. In this paper, the lithium ion was selected as the best recent choice to the vehicle industries based on its different characteristics [31, 32]. The studied battery cell characteristics is presented in Table 2.

The simplest model of a lithium ion cell equivalent circuit, which is the voltage source, linked in series with an internal resistance. The basis to define the lithium ion battery charging or discharging mode is the battery current sign [33].

In this study, we adopted the conventional $i \geq 0$ as a charging mode and $i \leq 0$ as a discharging mode. The battery pack used for the parallel HEV is 250 V formed by 76 cells in series and 56 cells in parallel. The charging and discharging mode were described by the following equations, respectively:

- Model of lithium ion battery voltage, in the charge time is described by equation (14) [34]:

$$U_{bat} = E_0 - R_i - K\frac{Q}{it+0.1Q}i^* - k\frac{Q}{Q-it}it + A\exp(-Bit) \quad (14)$$

- In the discharging time, the equation of the lithium ion battery voltage is described by the following equation (15) [34] :

$$U_{bat} = E_0 - Ri - K.\frac{Q}{Q-it}.i^* - k\frac{Q}{Q-it}.it + A\exp(-B.it) \quad (15)$$

- The SOC is the available state of the HEV that can be charging, discharging or remaining in idle state, defined by equation (16) [34] . Indeed, the energy state of the battery should not diverge from its lowest and highest limits 20% and 80% respectively.

$$SOC = 100(1-\frac{it}{Q}) \quad (16)$$

Where: E_0 is the battery constant voltage (V), R is the internal resistance (Ω), K is the Constant polarization (Ω), Q is the battery capacity (Ah), i is the battery current (A), it is the actual battery charge (Ah), i is the filtered current (A), A is the exponential zone amplitude (V), B is the exponential zone inverse constant time $(Ah)^{-1}$.

Table 2. Lithium ion cell (3.3 V, 2.3 Ah) characteristics.

Nomenclature	Values
E_0	3.366 V
R	0.01 Ω
K	0.0076 Ω
A	0.26422 V
B	26.5487 $(Ah)^{-1}$

2.6. Internal Combustion Engine modeling

The ICE type used in this application is the AIXAM MEGA thermal motor [35]. The engine's fuel consumption map is shown in Fig.4. The instantaneous fuel consumption $\dot{m}_{ice}(g/s)$ of the engine can be expressed as follows:

$$\dot{m}_{ice} = \frac{T_{ice}\Omega_{ice}b_e}{3.44\times10^{10}} \quad (17)$$

Where: $\dot{m}_{ice}$ is the mass of fuel consumed by the engine (g), Ω_{ice} is the engine speed (rpm), T_{ice} is the ICE motor torque $(N.m)$, b_e is the specific fuel consumption $(g/(Kw.h))$, and it can be found by a simple interpolation of the torque and speed in the engine map.

The instantaneous CO_2 emission of the ICE motor is determinate as follow:

$$\dot{m}_{CO2} = 2.65\frac{\dot{m}_{ice}}{\rho_{fuel}} \quad (18)$$

Where: ρ_{fuel} is the fuel density.

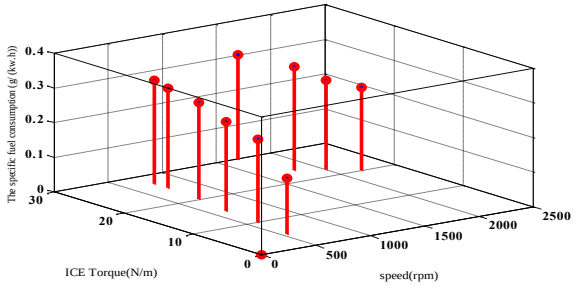

Fig.4. ICE specific fuel consumption.

In this study, the continuously variable transmission CVT model with reduction gear allows us to obtain the multiplication. It gives the freedom for the ICE motor to work at its most efficient level as demanded by the torque as detailed in Fig.5. The transmission models are generally simple models based on a reduction value [36] as presented in the following equations:

$$T_{cvt} = i_1 T_{ice} \quad (19)$$

$$\Omega_{ice} = i_1 \Omega_{cvt} \quad (20)$$

$$T_{ice1} = i_2 T_{cvt} \quad (21)$$

$$\Omega_{cvt} = i_2 \Omega_{mec} \quad (22)$$

Where: T_{cvt} is the CVT torque, T_{ice1} is the output torque of the gear, and Ω_{cvt} is the rotation speed of the CVT.

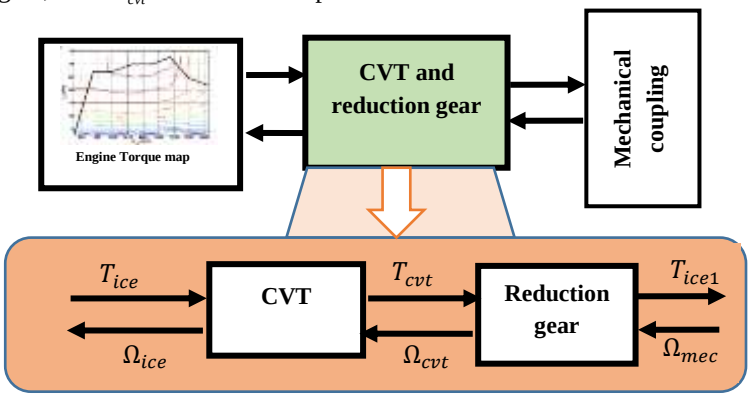

Fig.5. CVT and reduction gear model.

2.7. Driver Model

The driver model is used to imitate the different driver's manipulation of the acceleration and brake pedals. The driving cycle sends the demanded speed V_{ref} to the driver. According to comparison of this reference and the actual feedback speed V_{model}, the total reference force $F_{tot-ref}$ is calculated using PI regulator and sent to the vehicle control unit [37] as shown in Fig.6.

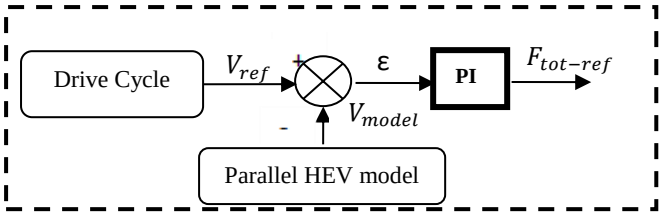

Fig.6. Driver model.

The proportional and integral gains respectively K_p and K_i associated to the used proportional integral controller PI according to the tuning method are defined by the following equations:

$$K_p = 2m\omega\xi \quad (23)$$

$$K_i = m\omega^2 \quad (24)$$

Where: ω is the pulsation of the system (rad/s) and ξ is the system damping coefficient.

3. Inversion Based Control

The parallel HEV control system was detailed in this section. For this study, we adopted the inversion control rules: to construct the control scheme, each relationship type in the parallel HEV model was reversed [38], since the proposed control must define this appropriate input $E_{ref}(t)$ from the desired output $S_{ref}(t)$, as described in Fig.7.

This study interested on the torque flow distribution between the different energy sources. Therefore, it is assumed that the braking torque is equal to zero.

3.1. Control of the Chassis

According to chassis model defined in equation (8), the control equation is presented as follows:

$$V_{model-ref} = \frac{1}{m}\int F_{tot-ref} - F_{res} \quad (25)$$

3.2. Wheels control

Inversing the model equation (3) we deduce the total reference torque $T_{tot-ref}$ represented in equation (26) and inversing the model equation (9) we deduce the reference mechanical speed of the parallel HEV wheels in equation (27):

$$T_{tot-ref} = F_{tot-ref} \times r \quad (26)$$

$$\Omega_{mec-ref} = \frac{V_{model-ref}}{r} \quad (27)$$

3.3. Mechanical coupling control

The mechanical coupling is the sum of the electric and thermal torques. Thus, the reference PMSM T_{em-ref} is fixed by the following equation:

$$T_{em-ref} = T_{tot-ref} - T_{ice1-ref} \quad (28)$$

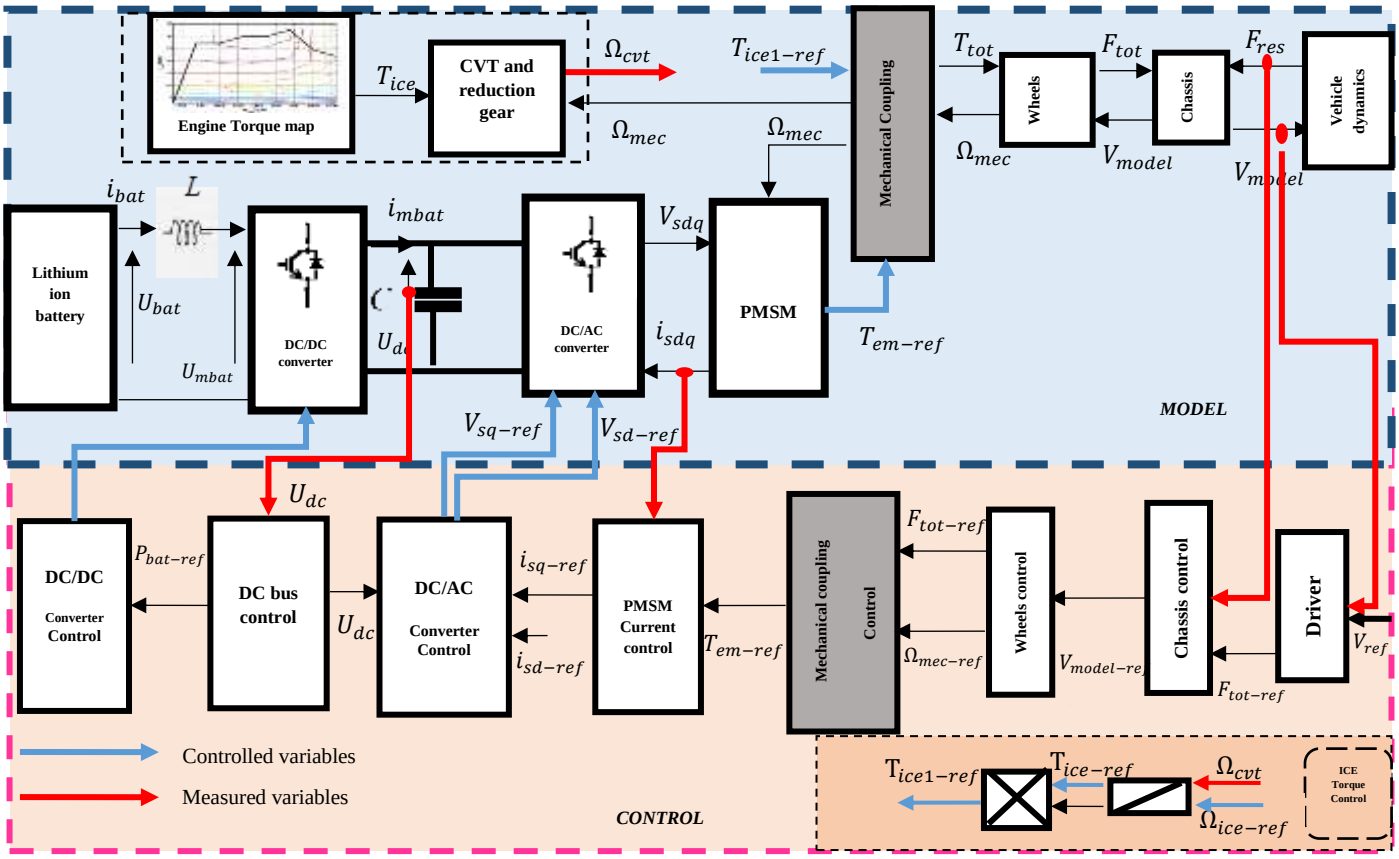

Fig.7. Parallel HEV control configuration.

3.4. ICE control

Different methods were developed in the literature studies to control the ICE. The first method consists in regulating the ICE at a given operating point by fixed reference torque $T_{ice-ref}$ and the reference speed $\Omega_{ice-ref}$ of the engine in order to ensure the operation of ICE in its zone of optimum efficiency. The second method is to use a couple's distribution factor to control the MSAP and the ICE at the same time. In this study, the ICE was controlled with the first strategy.

3.5. PMSM current control

The PMSM model presented in the d-q rotating Park frame (10) is controlled through the current controller. It includes a decoupling action and a proportional integral (PI) controller, which enables avoiding the residual steady state error between the reference and the output currents [13]. From the detailed MSAP model, we developed the stator currents control to determine the reference voltages in the d-q rotating Park models V_{sd-ref} and V_{sq-ref} as shown in Fig.8.

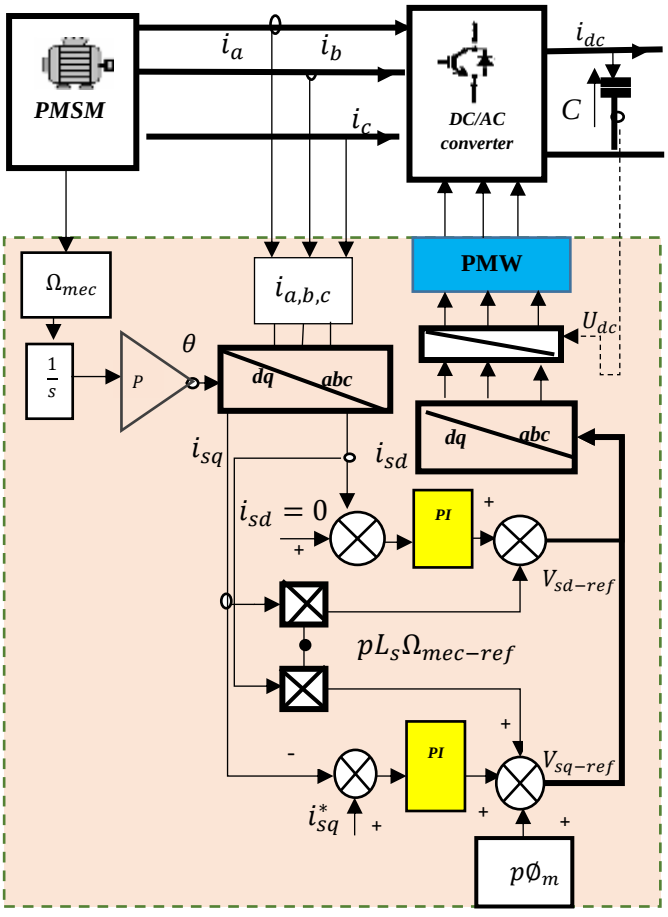

Fig.8. PMSM current control strategy.

3.6. Control of DC/AC converter

Voltages delivered by the converter depend on the control voltages of the converter V_{sd-ref} and V_{sq-ref}, given by the following equations:

$$V_{sd} = V_{sd-ref}\frac{U_{dc}}{2} \quad (29)$$

$$V_{sq} = V_{sq-ref}\frac{U_{dc}}{2} \quad (30)$$

3.7. DC bus control

To control the DC bus voltage as presented in Fig.9, the current flowing through the DC capacitor must be controlled. In fact, this voltage must be kept equal to U_{dc-ref} ensuring a balance between production and consumption. This control of the DC bus reference current i_{dc-ref} is ensured with a PI corrector as presented in equation (31):

$$i_{dc-ref} = PI(U_{dc-ref} - U_{dc}) \quad (31)$$

3.8. DC/DC converter Control

The control diagram structure of chopper is presented in Fig.9. As for the modulated voltage $U_{mbat-ref}$ of the converter control, it is expressed as follows:

$$U_{mbat-ref} = m_{bat-ref}U_{dc} \quad (32)$$

Where: $m_{bat-ref}$ is the control signal of the DC/DC converter.

3.9. Control of the storage system

The objective of this command is to adjust the current i_{bat} to its reference value $i_{bat-ref}$ with purpose controlling the charge and discharge of the battery, using a PI regulator as described in the following equation:

$$U_{bat} = PI(i_{bat-ref} - i_{bat}) \quad (33)$$

Figure 9 shows the control strategy of the storage system associated to the DC bus control.

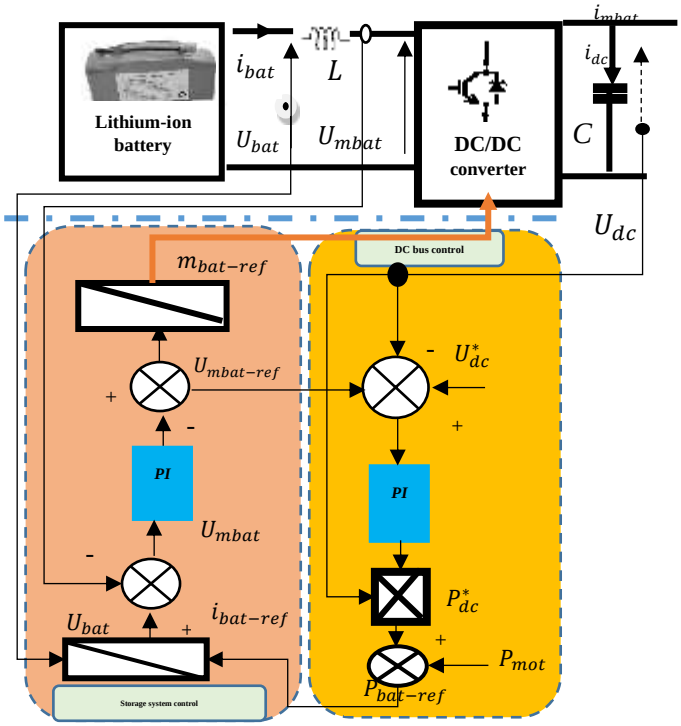

Fig.9. Storage system and DC bus control scheme.

4. Proposed Supervision Strategy

This study was executed to ensure the parallel HEV system autonomy on the road journey and to meet the established energy constraints. Then, the developed strategies associated to the power management supervisor requires the information's about the battery SOC and the vehicle speed to control the electric and thermal torques. Therefore, five operation modes can be distinguished: pure electric mode, hybrid mode, pure thermal mode, regenerative braking mode, and no power-transmitted mode, as shown in Fig.10.

Indeed, the energy transaction between the two energy sources was supervised according to the adequate mode designed from our proposed control strategy. During the vehicle proper functioning, the lithium ion battery is initially used as a storage/backup system until it is used out to shift to the ICE, ensuring a balance between the generated and consumed powers absorbed or injected into the battery. Thus, the power balance is expressed as follows:

$$P_{bat}(t) = P_{dem}(t) \quad (34)$$

This would help to fulfill the following conditions:

- Charging the battery from the deceleration phase and the regenerative braking.
- Minimizing the ICE operation in order to decrease the fuel consumption and CO_2 emission.
- Controlling the battery energy charged and discharged with lowest and highest limits to prohibit the overcharging and deep discharging of the battery, respectively.

The supervision algorithm is responsible for the operating mode switching and optimal power distribution to reduce the energy consumption of the HEV system. The supervision algorithm is practical, simple to implement and adequate. In fact, it provides a better split torque between the two motors based on the use of logic (If) to characterize each mode; then, it acts in a simple way in real time using the MATLAB/Simulink software.

Besides, the proposed strategy would act depending on the different information collected from the parallel HEV model. To this end, the supervision block receives this information as inputs:

- The reference speed of the parallel HEV.
- The acceleration phase of the vehicle.
- The deceleration phase of the vehicle.
- The battery SOC minimum bound limit of the parallel HEV.
- The battery SOC maximum bound limit of the parallel HEV.

Here the following modes of the used control strategy are explained:

- Electric mode (mode 1): If the HEV is in the acceleration phase, the vehicle speed is below the lower limit and the battery SOC is above the lower limit, then the ICE is turned OFF and the EM is turned ON. In this case: $(T_{tot-ref} = T_{em-ref})$.
- Hybrid mode (Mode 2): If the vehicle is in the acceleration phase, the vehicle speed is above the lower limit and the battery SOC is above the lower limit, then the ICE is turned ON and the EM is turned ON. In this case: $(T_{tot-ref} = T_{em-ref} + T_{ice1-ref})$.
- Thermal mode (mode 3): If the vehicle is in the acceleration phase and the battery SOC is below the minimum limit, then, the ICE is turned ON and the EM is turned OFF. In this case: $(T_{tot-ref} = T_{ice1-ref})$.
- Regenerative braking mode (mode 4): If the vehicle is in the deceleration phase and the battery SOC is below the maximum limit, then, the ICE is turned OFF and the EM is turned ON as a generator. In this case: $(T_{tot-ref} = T_{gen-ref})$.
- Mode 5: If the vehicle is in the deceleration mode and the SOC of the battery is above the maximum limit, then, the battery will not support the extra charge, and the energy will be dissipated as a heat form, which is not an adequate mode. In this case, there is no power transmitted and $T_{tot-ref} = 0$.

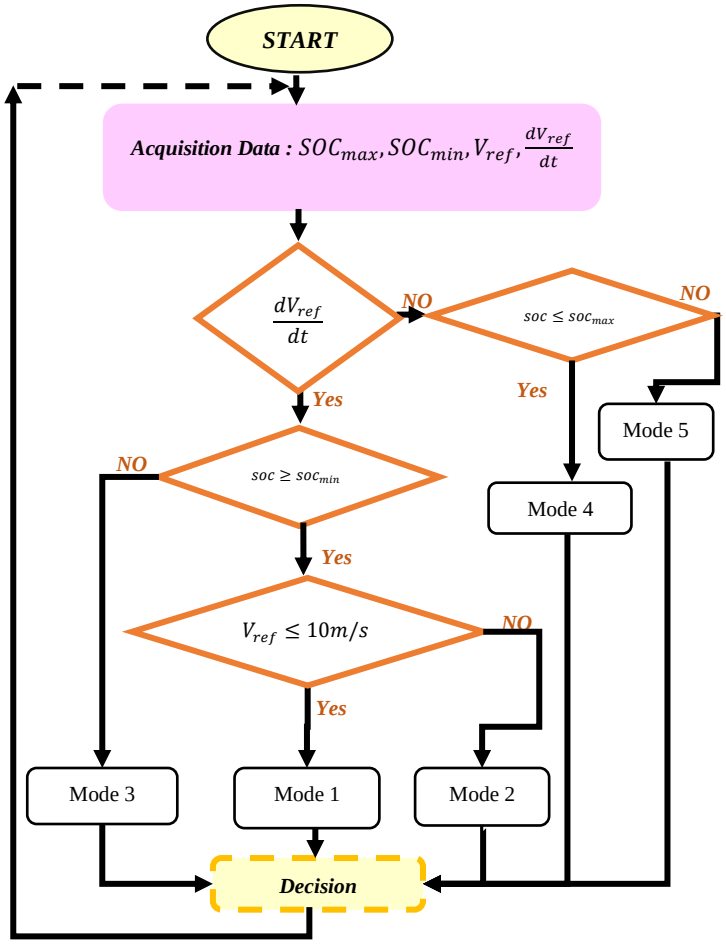

Fig.10. Structure of the proposed supervision and optimization algorithm.

5. Optimization Problem Formulation

After a deep study on the design, sizing and architectures, several researchers focused their research on the optimization of the different EV parameters. This was supported by the general research trend that emphasized optimization as the up-to-date trend in research. In this context, several optimization criteria have appeared in the literature: HEV cost, fuel consumption, electricity charging and CO_2 emission [39-42].

The parallel HEV system was studied considering the HEV lifetime, especially lifetime of the lithium ion battery, which was estimated at 10 years. To determine the optimum torque of electric and thermal motors needed to propel the parallel system, an optimization problem was developed. An economical criterion was chosen for this problem to reduce the total investment system cost. In the economic analysis, the total cost function C_T is defined as the sum of the electric charge costs C_e, the fuel consumption costs C_f and the components cost C_c.

5.1. Electric charge cost

The electric charge cost C_e includes the electricity buying cost ρ_{el} described by equation (35):

$$C_e(t) = \frac{\rho_{el}}{3600 \times 1000} \sum_{t=1}^{N} T_{em}(t)\Omega_{mec}(t) \quad (35)$$

Where, N is the drive cycle duration, $N \in \mathbb{R}$ and t is the simulation time.

5.2. Fuel consumption cost

The fuel consumption cost depends on the fuel cost ρ_f expressed by equation (36):

$$C_f(t) = \frac{\rho_f}{\rho_{LHV}} \sum_{t=1}^{N} T_{ice}(t)\Omega_{mec}(t) \quad (36)$$

ρ_{LHV} : is the lowest heating value of the fuel.

5.3. Components costs

The instantaneous components cost C_c is the sum of: PMSM motor cost C_{em}, ICE motor cost C_{ice} and lithium ion battery cost C_{bat} values, which depends on the vehicle lifetime t_{life} the drive cycle distance d, the yearly traveled distance t_d and the vehicle life time y_v of the vehicle, as given in equation (37):

$$C_c = \frac{d}{t_{life} \times t_d}\left(1 + r_i \frac{y_v + 1}{2}\right)\left(C_{bat} + C_{em} + C_{ice}\right) \quad (37)$$

Where: r_i is the yearly interest rate, which is equal to 5%.
The instantaneous cost function includes the fuel consumption cost, the electric charge cost and the cost of the total components. It is expressed by the following expression:

$$C_T(t) = \sum_{t=1}^{N} C_e(t) + C_f(t) + C_c(t) \quad (38)$$

5.4. Economic problem constraints

Since the energy management system of the parallel configuration of the HEV was achieved, the objective function defined previously is also subject of many constraints. These are divided into equality and inequality constraints as follows:

- The equality constraints ensure the balance of the demanded and provided powers at each instant. It is calculated using the following equation:

$$P_{dem} = T_{em}\Omega_{mec} + T_{ice1}\Omega_{mec}\eta_{ice} \quad (39)$$

Where: η_{ice} is the ICE efficiency.

- The inequality constraint of the system is calculated using the following equation:

$$T_{em}\Omega_{mec} + P_{loss} + P_{acc} \le P_{bat} \quad (40)$$

Where: P_{loss} is the PMSM power loss and P_{acc} is the HEV accessory power (radio, PS…).
The electric and thermal torques are bounded with minimal and maximal defined by:

$$T_{em\min} \le T_{em} \le T_{em\max} \quad (41)$$

$$T_{ice1\min} \le T_{ice1} \le T_{ice1\max} \quad (42)$$

Where: $T_{em\min}$ and $T_{ice1\min}$ are the minimum torques which can be produced by the electric and thermal motors, respectively. $T_{em\max}$ and $T_{ice1\max}$ are the maximum torques which can be produced by the electric and thermal motors, respectively.

6. Proposed Optimization Algorithms

The recent literature is interested in different optimization algorithms. However, many of the researchers are rather interested in a comparative study between the different proposed algorithms trying to achieve different purposes and vehicle architectures.

In this part, the different suggest energy management strategies structure was introduced. Two sections were introduced in this framework: the first part is the optimal energy management method design and defined control law calculation using the supervision method in real-time. The second part is an offline optimization formulation applied to the developed energy management method for the parallel HEV, which was achieved by the torque division and coordination control approach.

Depending on the initial conditions given to the control strategy, the parallel HEV follows a specific charging and discharging power profile so that it can contribute to the total drive cycle demand. Fig.11 shows the construction of the proposed parallel HEV energy management system.

In this paper, a study of an economic problem optimization for a parallel HEV system was investigated. For that, a comparison study of different optimization algorithms were implemented, tested and compared.

6.1. PSO

The PSO is an evolutionary algorithm that was suggested by Eberhart and shi [43]. It is characterized by its robustness, efficiency and simplicity of implementation with a few adjustable parameters [44]. Besides, it is appropriate for multiple objective optimization problems. Hence, the global optimal is given by the swarm optimizer thanks to the very easy rules of moving in the search area.

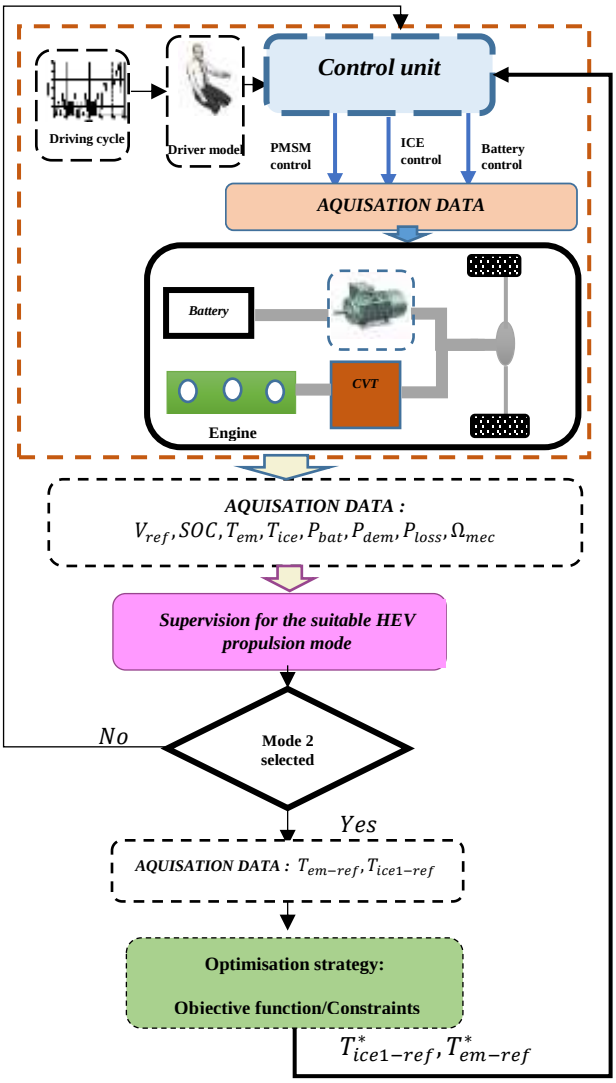

Fig.11. General energy management system configuration.

Here, the PSO algorithm can be described by the following formulation of the position $x(t)$ and the velocity $v(t)$ in equations (43) and (44), respectively:

$$x_i^{t+1} = x_i^t + v_i^{t+1} \quad (43)$$

$$v_i^{t+1} = \omega v_i^t + \alpha r_1 (g_{best} - x_i^t) + \beta r_2 (p_{best} - x_i^t) \quad (44)$$

Where: g_{best} is the global best of the swarm optimization, p_{best} is the best solution for each particle, ω is the inertia factor, $r_{1,2}$ is the uniformly distributed random number between 0 and 1, and α, β are the acceleration constants.

6.2. APSO

The APSO is an accelerated version of the PSO algorithm. Hence, it is characterized by its efficiency and high quality solution. In addition, it was known with its simplicity compared to the PSO algorithm [4]. The APSO is initialized with a group of random particles and then pursuit the optimal solution by updating generations. The particles are evaluated depending on some objective function criteria after each step. Each particle is dealt as a point in an N-dimensional space, which adjusts its 'flying' by its own experiment as well as the flying experiment of other particles via the reminder of the best earlier positions, velocity, and accelerations of itself and its neighbors. Then the particles start to shift towards the best neighbor's position before the flock gets an optimum of the fitness function. The position and velocity equations are presented as follows:

$$x_i^{t+1} = (1-\beta) x_i^t + \beta g_{best} + \alpha r \quad (45)$$

$$v_i^{t+1} = (1-\beta) v_i^t + \alpha r + \beta (g_{best} - x_i^t) \quad (46)$$

6.3. Convex

Convex optimization is a fast and reliable algorithm used to solve optimization problems and can be used through a MATLAB tool called « CVX » [45]. The optimal design and energy management enable finding a unique global minimum.

6.4. Genetic

GA is one of the most interesting optimization techniques, due to its good search performance and low complexity. It allows using different techniques inspired from evolutionary biology as the selection, mutation and crossover to solve a problem. The most popularly employed technique in this algorithm is to create a random individual group from a given population. So, the developed individuals are evaluated with the help of the studied evaluation function. Then an aptitude for the given context is put through the score received by the individuals. The best two individuals are then elected to create one or more offspring based on random mutations that were performed on the offspring [46].

6.5. Fmincon

It is a Nonlinear Programming optimization MATLAB tool available in the "Optimization toolbox". This function is adopted for non-linear problems [47].

7. Simulation Results

The model and control of HEV were realized with MATLAB/Simulink software using the different parameters presented in Table 1. To validate the model, control, and the performance of optimization algorithms, the overall system was simulated during the 1180 s. Thus, a verification must be executed on the same hardware-configured simulation platform. The simulation computer configuration used in this study is an Intel® Celeron® with a CPU 3867U, 1.80 GHz, and 4 Go memory capacity.

The normalized drive cycle used for this study is the NEDC drive cycle. This is the most used cycle in the research field, owing to the easy interpretation of its result. It is used in Europe and different other countries mainly to measure the consumption and polluting emissions of vehicles. The NEDC cycle is composed of two different parts: urban and extra-urban. The system, cycle and problem setting and parameters are given in Tables 3, 4, 5 and 6. Thus, P_{acc} of the parallel HEV system is estimated around 500 W.

Table 3. Algorithms parameters.

Parameter	Population size	Number of iterations	Variable number	Tolerance	Acceleration constants α,β	Inertia weight $\zeta_{1,2}$	Crossover	Migration
APSO	100	100	2	0.95	0.5	0.2/0.5	-	-
PSO	100	100	2	0.95	0.5	0.002/0.004	-	-
GA	100	100	2	-	-	-	0.9	0.2
Convex	100	100	2		-	-	-	-
Fmincon	100	100	2	0	-	-	-	-

Table 4. NEDC cycle parameters.

Parameters	Values
Distance (m)	11023
Mean speed(m/s)	33.6
Duration(s)	1180

Table 5. Parallel HEV component cost.

Components of HEV	Costs (DT)
EM	15387
Battery	1387.68
ICE	11599

Table 6. Boundaries values.

Variables (N.m)	Values
$T_{em\min}$	0
$T_{em\max}$	340
$T_{ice1\min}$	0
$T_{ice1\max}$	120

Figure 12 to Fig.22 presents the results of the parallel HEV system control.

In facts, The NEDC cycle evolution is presented in Fig.12. Thus, we can remark that the model speed follows the drive cycle speed perfectly with small errors during transitions.

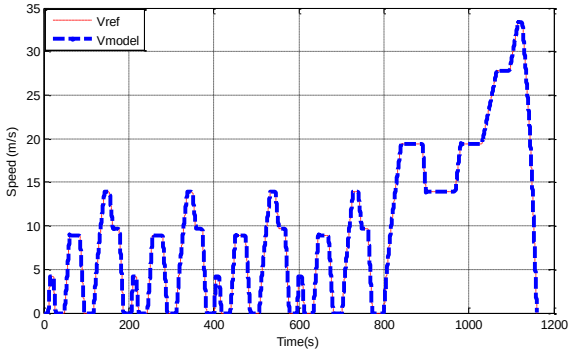

Fig.12. Drive cycle speed.

The electromagnetic torque of the PMSM and the ICE torque evolutions during the NEDC cycle are illustrated in Fig.13.

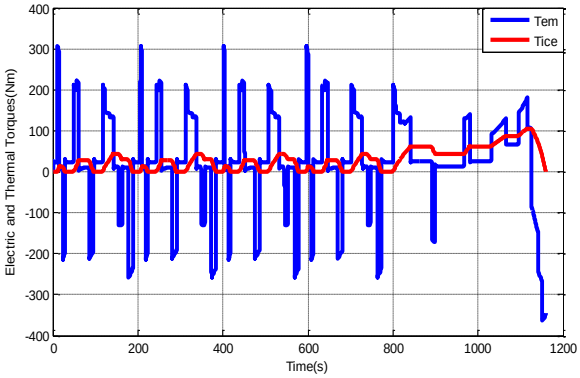

Fig.13. PMSM and ICE torques.

The mechanical speed of the hybrid system evolution during the NEDC cycle is illustrated in Fig.14.

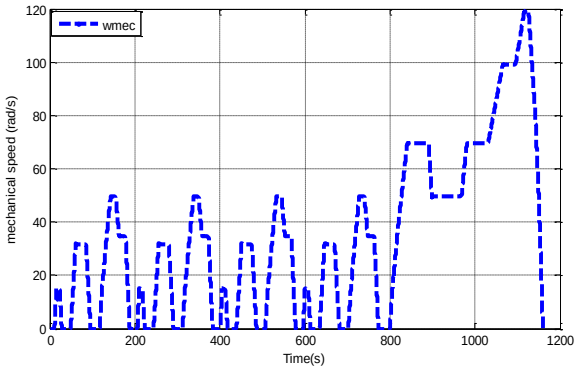

Fig.14. Mechanical speed.

Figure 15 shows the dynamics of the system power demand during the cycle. The chosen convention in this work demonstrate that the negative powers correspond to the charging mode which the HEV battery store energy regenerative brake mode. However, the positive powers were selected to the discharging mode of the HEV lithium ion battery to propel the PMSM motor.

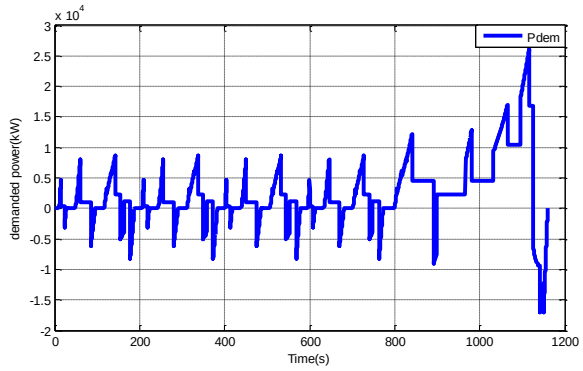

Fig.15. Power demand.

The references direct and quadrature currents evolutions used in the current control of the PMSM motor are displayed in Fig. 16.

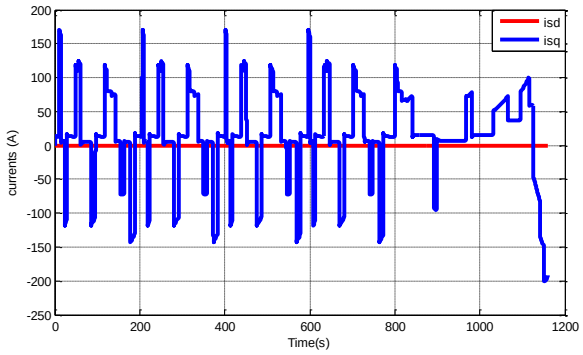

Fig.16. Direct and quadrature current.

The lithium ion battery current and SOC curves are presented in Fig.17 and Fig.18, respectively. These results affirm the selected convention in which negative currents are dedicated for the discharging cases and the positive ones for the charging cases.

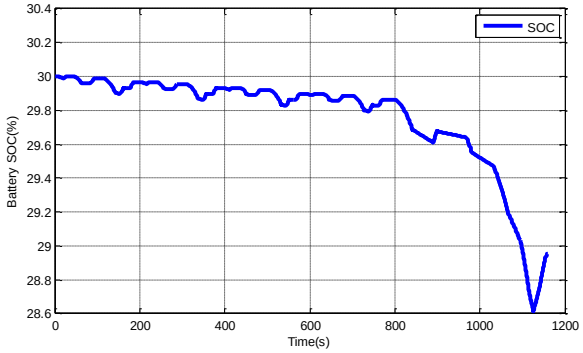

Fig.17. Lithium ion battery SOC.

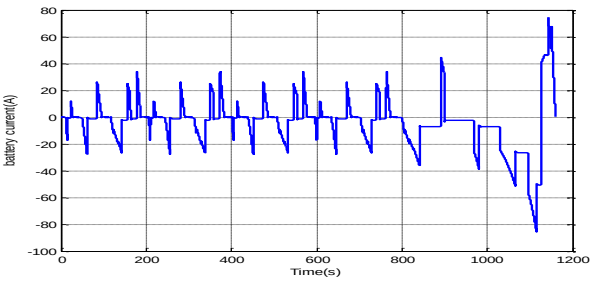

Fig.18. Lithium ion battery current.

On the other hand, the used PMSM efficiency during this simulation performance is shown in Fig.19. We can remark that the total efficiency of the motor between 0 and 1180 seconds does not exceed 35% of the total efficiency of its system.

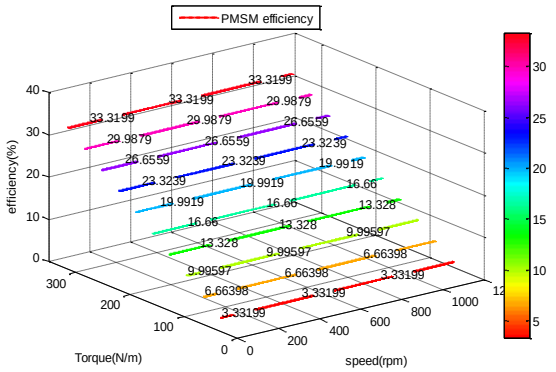

Fig.19. PMSM efficiency map.

The energy balance between the different system components, especially the storage system, allows the adjustment of the DC bus voltage and its maintenance at its reference value, which is equal to 500 V as shown in Fig.20.This figure shows the effectiveness of the designed control.

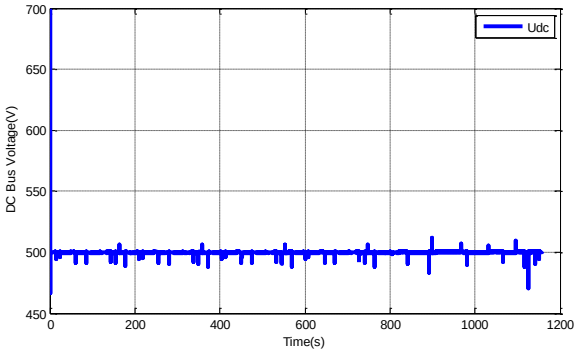

Fig.20. DC bus voltage.

The total torque evolution of the hybrid system under the NEDC cycle is shown in Fig.21.

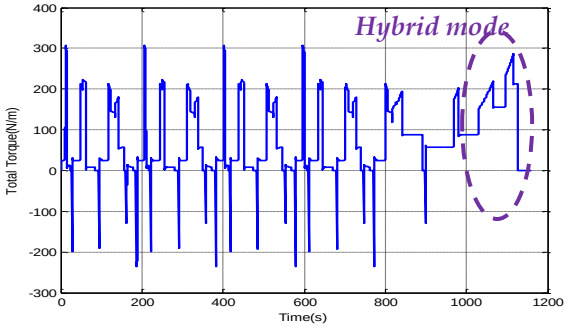

Fig.21. Total torque.

According to the algorithm for the supervision strategy explained in section 4, the five operating modes of the parallel HEV were recognized. Figure 22 displays the transitions between five different modes respectively. This figure shows

the effectiveness of the studied control management supervisor following the profiles of each operating mode.

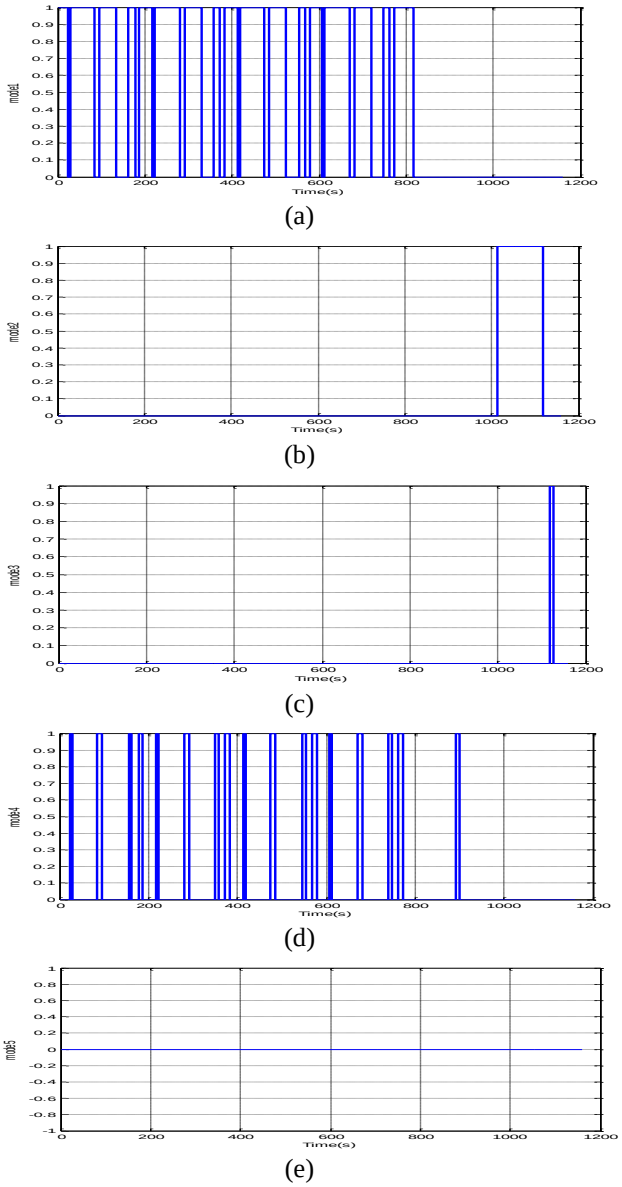

(a) (b) (c) (d) (e)

Fig.22. Different operating modes: (a): electric mode, (b): hybrid mode, (c): thermal mode, (d): regenerative braking mode and (e): no power transmitted

To evaluate the performance and validity of the different offline optimization algorithms structure, the results were analysed under the NEDC cycle. In this part our simulations focused on the hybrid mode of the vehicle where (both of) the electric motor and engine are used to propel the vehicle simultaneously in the interval [1014 s, 1160 s].

The results for the optimized electric torque using PSO, Fmincon, APSO, GA and Convex energy management algorithms in the hybrid mode of the vehicle are displayed in Fig.23. As for the results of the thermal torque, they are displayed in Fig.24.

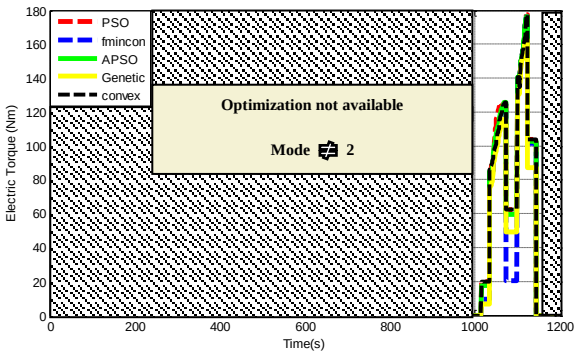

Fig.23. Optimized electric torques under different optimization algorithms in the hybrid mode.

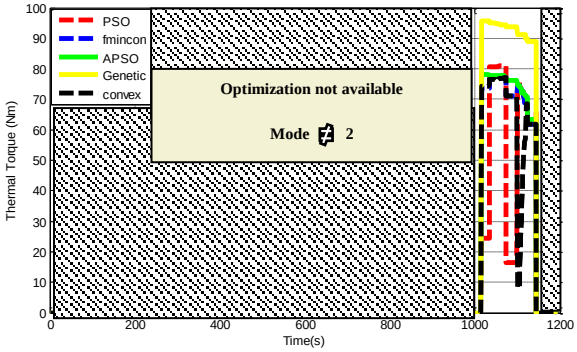

Fig.24. Optimized thermal torques under different optimization algorithms in the hybrid mode.

The simulations were also carried out for the fuel consumption minimization and their results as well as those of the CO_2 emission reduction are shown in Fig. 25 and Fig.26, respectively.

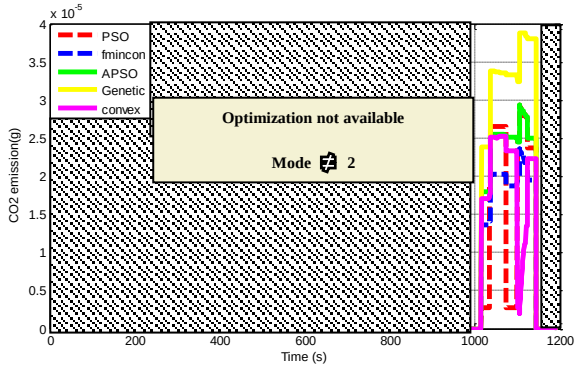

Fig.25. Fuel consumption evolution in the hybrid mode.

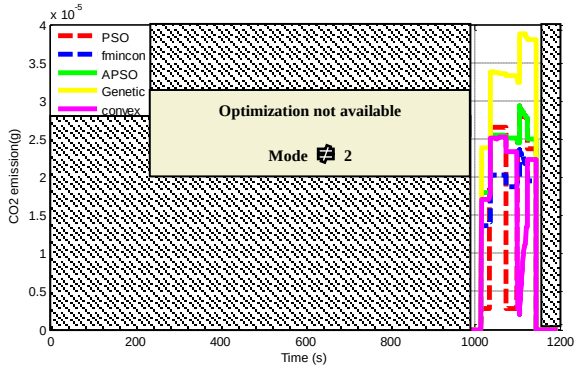

Fig.26. CO_2 emission evolution in the hybrid mode.

For a better understanding of the optimization torques changeable values in the time interval [1014 s, 1160 s], the battery SOC profiles of the different energy management strategies for the parallel HEV mentioned above are presented in Fig.27. We remark, in the interval of [1014 s, 1160 s] corresponding to the hybrid mode interval of the propulsion system, the SOC decrease for the different algorithms depends on the HEV electricity consumption and the increase of the electric torque.

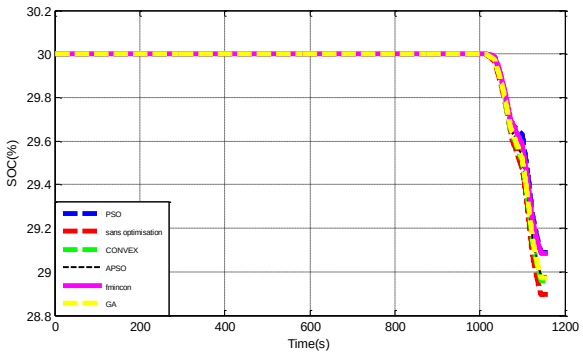

(a)

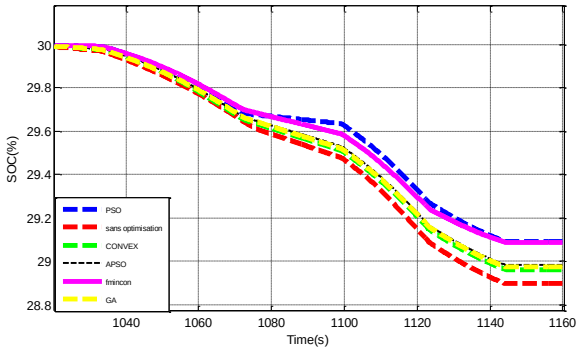

(b)

Fig.27. (a) SOC evolution in the hybrid mode with the different optimization algorithms, (b) zoomed view.

The resulting control sequences are shown in Fig.28 and Fig.29, whereas the numerical results are given in Table 7.

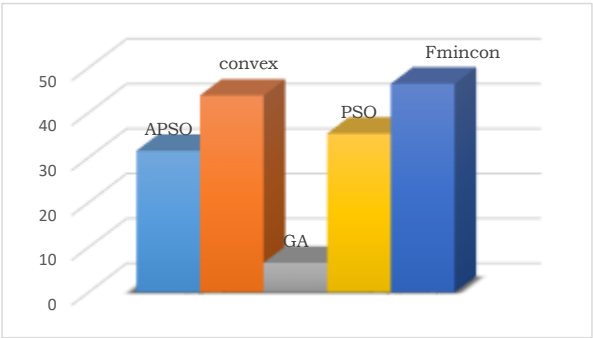

Fig.28. Percentage of reduction of fuel consumption and CO_2 reduction.

Figure 28 shows a comparison of the reduction percentage of the fuel consumption and CO_2 emissions of each algorithm.

It is important to notice that the parallel HEV extensively satisfies the European light-duty vehicle emissions legislation referring to the NEDC. Taking into consideration the mean values of the different optimizations methods, the emissions caused by the HEV are also lower than 95 gCO_2/km [48].

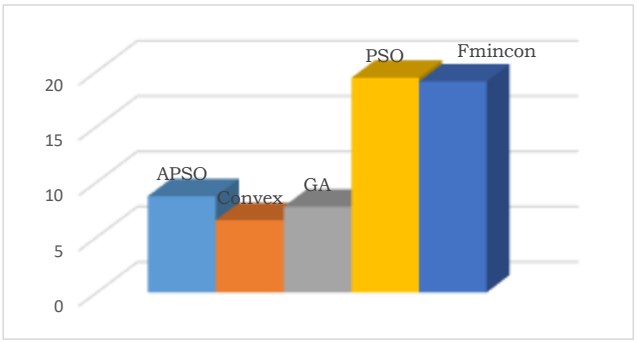

Fig.29. Charge sustaining operation enhancement.

Figure 29 also shows a comparison of the charge sustaining operation enhancement percentage for the lithium ion battery of each algorithm.

When comparing the simulation performances of the used offline approaches, it is clear that the proposed algorithms are run over 100 independent times and the collected statistical results are precise in Table 7. This table reveals the best instantaneous fuel consumption, CO_2 emission, reduction and improvement percentages results, CPU computational time, best cost and best iteration, respectively for each optimization experiment. Hence, the reduction in fuel consumption for the non-optimal case was calculated relative to the optimal hybrid case.

However, the results described in Table 7 can direct the user towards the best choice of the appropriate optimization algorithm according to his prefixed objective.

It is clear that Fmincon and convex optimization algorithms show a higher minimization in both fuel consumption and CO_2 emission when compared to the PSO, APSO and GA results that achieved only 35.34%, 31.49% and 6.53%, respectively.

For the lithium ion battery sustaining charge enhancement, the PSO and the Fmincon optimization algorithms have the highest results. Indeed, the above-mentioned algorithms are by far better than the APSO, Convex and GA results that achieved 8.69%, 6.54% and 7.76%, respectively.

The simulation time is also another substantial parameter for real-time applications. The computation time based on Fmincon is non-competitive as it was capable to perform the energy sharing in the lowest time interval of 3.1 s.

Contrariwise, the APSO has the highest time interval performance with 58.40 s. The GA follows with 40.48 s, and then comes the convex algorithm with 32.4 s and the PSO algorithm with an average simulation time of 25.29 s.

Table 7. Optimization algorithms results.

Algorithms	Instantaneous fuel consumption (g/s)	CO_2 emission (g)	Reduction (%)	CPU (s)	Best Cost (DT)	Charge sustaining operation enhancement (%)
APSO	5.29e-07	1.65e-06	31.49	58.40	2.1315e+05	8.69
Convex	4.17e-07	1.30e-06	43.79	32.4	2.1315e+05	6.54
GA	7.15e-07	2.23e-06	6.53	40.84	2.1315e+05	7.76
PSO	5.03 e-07	1.57e-06	35.34	25.29	2.1315e+05	19.41
Fmincon	4.08 e-07	1.27e-06	46.43	3.51	2.1314e+05	19.07

This system should also ensure that the studied algorithms converge to the cheapest optimal solution at a fast speed. Figure 30 exhibits the relationship between optimal fitness and iteration number after 100 iterations achieved by the GA, PSO, APSO, Convex and Fmincon optimizations algorithms. When the cost function is small and remains unchanged, the optimal value of the different algorithms is considered to be the global optimal solution. Figure 30e shows that, when the iteration reached 10 generations, the fitness tended to be stable with the Fmincon algorithm. However, as can be seen from Fig.30a the fitness function tended to be stable starting from the 50th iteration using the APSO, and the 30th iteration using the PSO algorithm, Fig.30b. Figure 30c highlights that the GA algorithm converges to a minimum value of the cost function after more than 80 iterations. A closer look to the Fig.30d proves that the Convex algorithm converges directly to the minimum value of the cost function.

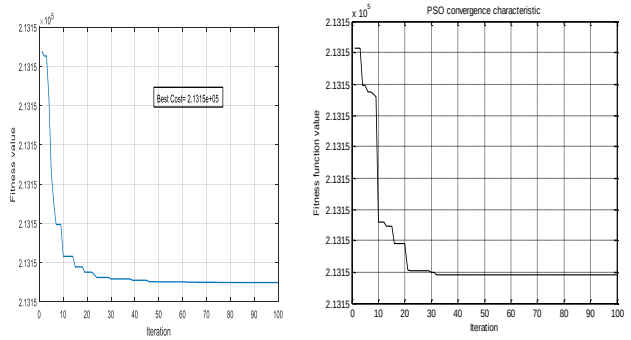

(a) (b) (c) (d)

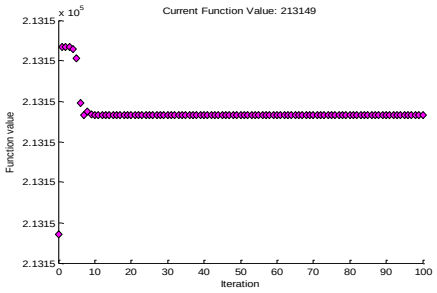

(e)

Fig.30. Best fitness functions: (a): APSO, (b): PSO, (c): GA, (d): Convex and (e): Fmincon.

8. Conclusion

This article developed a comparative study of different optimal control management strategies of a parallel HEV system under NEDC cycle. The different offline managements were carried out aiming to decrease the fuel consumption and CO_2 emission mainly in the hybrid mode where the electric and thermal motors propelled the vehicle simultaneously at high speeds. In addition, computational time was considered as an essential performance criterion. In the first section of the suggested energy management study, a supervision strategy was developed to manage energy flows between the electric and thermal motors. Then, the supervisor takes its decision to select the adequate operating mode to ensure the continuous supply of energy to propel the parallel HEV and maintain the state of charge of the battery at an adequate level. The second part consists of different offline algorithms that achieve an optimal split of the two motors while minimizing fuel consumption and CO_2 emission and maintaining the battery health. An economic assessment has been conducted by employing the total ownership cost for 10 years respecting different physical components constraints. Therefore, the optimization algorithms have been executed using a cost function. The principal objective was to satisfy all the constraints with minimum total cost.

Our simulation results have proven the efficiency of the PSO, APSO, GA, Fmincon, and Convex algorithms. However, each of the algorithms has different advantages and drawbacks concerning this model and simulation performances. For instance, the Fmincon, convex, PSO, and APSO were able to achieve better results on consumption reduction and CO_2 emission compared to the GA. However, the GA, PSO, Fmincon, and Convex achieved less computational time compared to the APSO.

Appendix

The Power losses of the PMSM is described by the equation as follows [21]:

$$P_{loss}(\Omega_{mec}, T_{em}) = c_1(\Omega_{mec})T_{em}^2 + c_2(\Omega_{mec})T_{em} + c_3(\Omega_{mec}) \quad (41)$$

Where the coefficients: $C_1 \geq 0$, C_2 and C_3 are function of the electric motor speed. According to Ω_{mec} the coefficients are calculated basing on two different methods: least square method and linear interpolation method [49].

References

[1] MH. Khooban, "Hardware-in-the-loop simulation for the analyzing of smart speed control in highly nonlinear hybrid electric vehicle", Transactions of the Institute of Measurement and Control, vol.41, pp. 458-467, 2019.

[2] MB. Ali, M. Elloumi, and G. Boukettaya, "Review on optimization algorithms for plug in hybrid electric vehicle", 19th International Conference on Sciences and Techniques of Automatic Control and Computer Engineering, Sousse, Tunisia, pp. 134-139, 24-26 March 2019.

[3] M. T. Elsir, M. A. Abdulgalil, A. T. Al-Awami, and M. Khalid, "Sizing and Allocation for Solar Energy Storage System Considering the Cost Optimization", 8th International Conference on Renewable Energy Research and Applications (ICRERA) ,pp. 407-412, November 2019.

[4] I. Rahman, PM. Vasant, and BSM. Singh, "On the performance of accelerated particle swarm optimization for charging plug-in hybrid electric vehicles", Alexandria Engineering Journal, vol. 55, pp. 419-426, 2016.

[5] S. Gherairi, "Zero-Emission Hybrid Electric System: Estimated Speed to Prioritize Energy Demand for Transport Applications", International journal of smart grid (ijsmartgrid) , December 2020.

[6] H. Arima,Y. Mizuno, N. Matsui, and F. Kurokawa "Model Based Design of Smart Grid System Based on Automotive System", 8th International Conference on Smart Grid (icSmartGrid) ,pp. 198-202, June 2020.

[7] G. Boukettaya, and L. Krichen, "A dynamic power management strategy of a grid connected hybrid generation system using wind", photovoltaic and Flywheel Energy Storage System in residential applications, vol. 71, pp. 148-159, 2014.

[8] M. Elloumi, R. Kallel, and G. Boukettaya, "Multi agent system design for PV integrated home management", International Journal of Renewable Energy Research, vol. 8, pp. 561-574, 2018.

[9] IEA, "Global EV Outlook 2019—Scaling-Up the Transition to Electric Mobility", IEA, London, UK, 2019.

[10] H. Li, X. Hu, and B. Fu, "Effective optimal control strategy for hybrid electric vehicle with continuously variable transmission", Advances in Mechanical Engineering, vol. 11, pp. 1687814018824811, 2019.

[11] T. Bunsen, P. Cazzola, and M. Gorner, "Global EV Outlook Towards cross-modal electrification", International Energy Agency, 2018.

[12] H. Guo, Q. Sun, and C. Wang, "A systematic design and optimization method of transmission system and power management for a plug-in hybrid electric vehicle", Energy, vol. 148, pp. 1006-1017, 2018.

[13] A. Gao, X. Deng, M. Zhang, and Z. Fu, "Design and validation of real-time optimal control with ECMS to minimize energy consumption for parallel hybrid electric vehicles", Mathematical Problems in Engineering, vol. 2017, 2017.

[14] J. Fu, S. Song, and Z. Fu, "Design of coordinated control strategy during driving mode switching for parallel hybrid electric vehicles", Transactions of the Institute of Measurement and Control, vol.41, pp. 2507-2520, 2019.

[15] R. Koubaa, "Double layer metaheuristic based energy management strategy for a Fuel Cell/Ultra-Capacitor hybrid electric vehicle", Energy, vol. 133, pp. 1079-1093, 2017.

[16] Y. Qiao, Y. Song, and K. Huang, "A Novel Control Algorithm Design for Hybrid Electric Vehicles Considering Energy Consumption and Emission Performance", Energies, vol. 12, pp. 2698, 2019.

[17] B. Xu, F. Malmir, D. Rathod, and Z. Filipi, "Real-time reinforcement learning optimized energy management for a 48V mild hybrid electric vehicle", SAE Technical Paper, 2019-01-1208, 2019.

[18] R. Xiao, B. Liu, and J. Shen, "Comparisons of energy management methods for a parallel plug-in hybrid electric vehicle between the convex optimization and dynamic programming Applied Sciences , vol. 8, pp. 218, 2018.

[19] M. Pourabdollah, N. Murgovski, and A. Grauers, "An iterative dynamic programming/convex optimization procedure for optimal sizing and energy management of PHEVs", IFAC Proceedings Vol. 47(3), pp. 6606-6611, 2014.

[20] J. Nellen, B. Wolters, L. Netz, S. Geullen, and E.Abraham, "A Genetic Algorithm based Control Strategy for the Energy Management Problem in PHEVs", GCAI, pp. 196-214, 2015.

[21] M. Pourabdollah, E. Silvas, and N. Murgovski, "Optimal sizing of a series PHEV: Comparison between convex optimization and particle swarm optimization", IFAC-Papers On Line, vol. 48, pp. 16-22, 2015.

[22] Z. Wang, B. Huang, and W. Li, "Particle swarm optimization for operational parameters of series hybrid electric vehicle", Proceedings of the 2006 IEEE International Conference on Robotics and Biomimetics, Kunming, pp. 682-688, 17 – 20 December 2006.

[23] S. Amaran, NV. Sahinidis, and B. Sharda, "Simulation optimization: a review of algorithms and applications", Annals of Operations Research, vol.240, pp. 351-380, 2016.

[24] X. LÜ, Y. WU, and J. LIAN, "Energy management of hybrid electric vehicles: A review of energy optimization of fuel cell hybrid power system based on genetic algorithm. Energy Conversion and Management", vol. 205, p. 112474, 2020.

[25] A. Gao, X. Deng, M. Zhang, and Z. Fu, "Design and validation of real-time optimal control with ECMS to minimize energy consumption for parallel hybrid electric vehicles", Mathematical Problems in Engineering, vol. 2017, 2017.

[26] X. Wu, B. Cao, X. Li, J. Xu, and X. Ren, "Component sizing optimization of plug-in hybrid electric vehicles", Applied energy, vol. 88, pp. 799-804, 2011.
[27] T. Nüesch, A. Cerofolini, and G. Mancini, "Equivalent consumption minimization strategy for the control of real driving NOx emissions of a diesel hybrid electric vehicle", Energies, vol. 7, pp. 3148-3178, 2014.
[28] ME. Hmidi, I. Ben Salem, and L. ElAmraoui, "Design and simulation of a 2DOF PID controller based on particle swarm optimization algorithms for a thermal phase of hybrid vehicle", International Journal of Engineering & Technology, vol. 7, pp. 506-511, 2018.
[29] Y. Krim, D. Abbes, and S. Krim, "Classical vector, first-order sliding-mode and high-order sliding-mode control for a grid-connected variable-speed wind energy conversion system: A comparative study", Wind Engineering, vol.42, pp. 16-37, 2018.
[30] MM. Hoque, MA. Hannan, and A. Mohamed, "Charging and discharging model of lithium-ion battery for charge equalization control using particle swarm optimization algorithm", Journal of Renewable and Sustainable Energy, vol. 8, pp. 065701, 2016.
[31] L. Barote, and C. Marinescu, " Li-Ion energy storage capacity estimation in residential applications with EV", 8th International Conference on Renewable Energy Research and Applications (ICRERA) ,pp. 326-330, November 2019.
[32] MB. Ali, M. Elloumi, and G. Boukettaya, "Modelling, Control, and Simulation of Parallel PHEV Powertrain System", 4th International Conference on Recent Advances in Electrical Systems, Hammamet, Tunisia, pp. 53-58, 23-25 December 2019.
[33] F. M. Ibanez, T. Ahmed, L. Idrisov, and J. S. Gutierrez, "An Impedance Based Modeling Towards the Aging Prediction of Lithium-Ion Battery for EV Applications", 8th International Conference on Renewable Energy Research and Applications (ICRERA) , pp. 146-151, November 2019.
[34] S. Khemakhem, M. Rekik, and L. Krichen, "A collaborative energy management among plug-in electric vehicle, smart homes and neighbors' interaction for residential power load profile smoothing", Journal of Building Engineering, vol. 27, pp. 100976, 2020.
[35] D. Loukakou, C. Espanet, and F. Dubas, "Modélisation, Conception et Expérimentation d'un véhicule hybride léger pour usages urbains", Thèse de doctorat.Université de Franche-Comté, Français, 2012.
[36] M. Yao, D. Qin, and X. Zhou, "Integrated optimal control of transmission ratio and power split ratio for a CVT-based plug-in hybrid electric vehicle", Mechanism and Machine Theory, vol. 136, pp. 52-71, 2019.
[37] J. Zhang, F. Xu, and Y. Zhang, "ELM-based driver torque demand prediction and real-time optimal energy management strategy for HEVs", Neural Computing and Applications, pp. 1-19, 2019.
[38] A. Pam, A. Bouscayrol, and P. Fiani, "Integration of the Road Slope in the Optimization of the Energy Management Strategy of a parallel HEV", IFAC-Papers OnLine, vol. 52, pp. 28-33, 2019.
[39] Y. Wang, X. Jiao, and Z. Sun, "Energy management strategy in consideration of battery health for PHEV via stochastic control and particle swarm optimization algorithm", Energies, vol. 10, pp. 1894, 2017.
[40] H. Jiang, L. Xu, and J. Li, "Energy management and component sizing for a fuel cell/battery/supercapacitor hybrid powertrain based on two-dimensional optimization algorithms", Energy, vol. 177, pp. 386-396, 2019.
[41] ELV. Eriksson, and EM. Gray, "Optimization of renewable hybrid energy systems–A multi-objective approach", Renewable energy, vol. 133, pp. 971-999, 2019.
[42] X. Hu, X. Zhang, and X. Tang, "Model predictive control of hybrid electric vehicles for fuel economy, emission reductions, and inter-vehicle safety in car-following scenarios", Energy, vol. 196, pp. 117101, 2020.
[43] Y. Shi, "Particle swarm optimization: developments, applications and resources", congress on evolutionary computation, Seoul, South Korea, South Korea, pp. 81-86, 27-30 May 2001.
[44] I. Darwich, I. Lachhab, and L. Krichen, "Implementation of an on-line multi-objective particle swarm optimization controllers gains self-adjusted of FC/UC system devoted for electrical vehicle", International Journal of Hydrogen Energy, vol. 44, pp. 28262-28272, 2019.
[45] M. Grant, and Boyd, "CVX: Matlab software for disciplined convex programming", version 2.1, 2014.
[46] X. Lü, Y. Wu, and J. Lian, "Energy management of hybrid electric vehicles: A review of energy optimization of fuel cell hybrid power system based on genetic algorithm", Energy Conversion and Management, vol. 205, pp. 112474, 2020.
[47] D. Abbes, A. Martinez, and G. Champenois, "Étude d'un système hybride éolien photovoltaïque avec stockage : Dimensionnement et analyse du cycle de vie", European Journal of Electrical Engineering (EJEE), vol.15/5, pp. 479-497, 2012.
[48] P. Update, "emission standards for passenger cars and light commercial vehicles, policy", International council clean transportation, 2014.
[49] M. Pourabdollah, N. Murgovski, and A. Grauers, "Optimal sizing of a parallel PHEV powertrain", IEEE Transactions on Vehicular Technology", vol.62, pp. 2469-2480, 2013.